

# International Conference on Space Optics—ICSO 2022

Dubrovnik, Croatia

3–7 October 2022

*Edited by Kyriaki Minoglou, Nikos Karafolas, and Bruno Cugny,*



## *CLICK Mission Flight Terminal Optomechanical Integration and Testing*



# CLICK Mission Flight Terminal Optomechanical Integration and Testing

William Kammerer<sup>\*a</sup>, Peter Grenfell<sup>\*a</sup>, Laura Hyest<sup>e</sup>, Paul Serra<sup>a</sup>, Hannah Tomio<sup>a</sup>, Nick Belsten<sup>a</sup>, Charles Lindsay<sup>a</sup>, Ondrej Čierny<sup>a</sup>, Kerri Cahoy<sup>a</sup>, Myles Clark<sup>b</sup>, Dani Coogan<sup>b</sup>, John Conklin<sup>b</sup>, David Mayer<sup>c</sup>, Jan Stupl<sup>c</sup>, and John Hanson<sup>d</sup>

<sup>a</sup>Massachusetts Institute of Technology, Department of Aeronautics and Astronautics, 77 Mass. Ave., Cambridge, MA 02139, USA

<sup>b</sup>University of Florida, Department of Mechanical Aerospace Engineering, 231 MAE-A, P.O. Box 116250, Gainesville, FL 32611, USA

<sup>c</sup>NASA Ames Research Center, Moffett Blvd., Mountain View, CA 94035, USA

<sup>d</sup>CrossTrac Engineering, 2730 Saint Giles Ln., Mountain View, CA 94040-4437, USA

<sup>e</sup>Institut Supérieur de l'Aéronautique et de l'Espace, 10 Av. Edouard Belin, 31400 Toulouse, France

## ABSTRACT

The CubeSat Laser Infrared Crosslink (CLICK) mission is a technology demonstration of a low size, weight, and power (SWaP) crosslink optical communication terminal. The 3U CLICK-A spacecraft is the first phase of the mission with a 1.2U optical communication downlink terminal. The twin 3U CLICK-B/C spacecraft are the second phase of the mission each with a 1.5U crosslink optical communication transceiver terminal.

This work discusses the flight functional and environmental testing for the CLICK-A terminal as well as the optomechanical design and testing for the CLICK-B/C terminals. The CLICK-A terminal serves as a risk reduction effort for the CLICK-B/C terminals, whose goal is to establish a 20 Mbps intersatellite link at separations from 25 to 580 km. The CLICK-B/C terminals communicate with M-ary pulse position modulation (PPM) using a 200 mW erbium-doped fiber amplifier (EDFA). The payloads are capable of ranging up to a precision of 50 cm. CLICK-B & C will both be deployed from the International Space Station (ISS) at the same time and fly in the same orbital plane.

We begin by discussing the final integration and environmental testing results from the CLICK-A terminal, which was launched to the ISS in July 2022 and expected to be deployed in September 2022, as well as preparation of the CLICK optical ground station in Westford, MA. Second we present the CLICK-B/C flight terminal development. We describe the optomechanical design of the optical bench and its interface with the terminal. A prototype optical bench with the initial version of the CLICK-B/C optomechanical design has been built and tested. We also capture the lessons learned that have informed the building of an engineering development unit (EDU).

**Keywords:** laser, optical, crosslink, intersatellite, communications, free space optical communication, CubeSat, pulse position modulation

## 1. INTRODUCTION

The miniaturization and commercialization of spacecraft electronics has enabled highly capable small satellites to be designed, built, and operated. These small satellites have capabilities once only possible by satellites much larger in size and mass.<sup>1</sup> Certain types of sensing, such as hyperspectral and high-resolution Earth imaging, can generate data at rates that are difficult to manage with current CubeSat communication capabilities. Optical communication offers many advantages over traditional radio frequency (RF) communication. Optical

\* These authors contributed equally to this work.

Further author information: (Send correspondence to W.K.)

W.K.: E-mail: wi26858@mit.edu

communication can support data rates orders of magnitude greater than RF communication with similar size, weight, and power (SWaP).<sup>2</sup> The directed nature of the beam means transmitters need less transmitting power over a specified distance to close a link. The narrow beam also improves security as it is more difficult to intercept.<sup>3</sup> Small satellite optical communication terminals are able to leverage components for the terrestrial fiber internet to reduce their SWaP.<sup>4</sup> The optical spectrum provides THz of unregulated spectrum for future high-bandwidth sensor payloads. Optical communication also supports precision time transfer and ranging which is important for future small multi-satellite missions.<sup>5</sup> However, clouds and weather are an issue due to their attenuation of the transmitted signal, and motivate optical space crosslink relays as well as low-cost portable optical ground stations.<sup>6</sup> CubeSat RF crosslink communications are utilized and have been also shown to significantly reduce latency for small satellites<sup>7</sup> but lack the high bandwidth offered by optical communications.

## 1.1 CLICK Mission Overview

The CubeSat Laser Infrared Crosslink (CLICK) mission is a two-phase demonstration to advance the state of the art in free space optical communication by demonstrating optical crosslinks and precision ranging between miniaturized optical transceivers flying on nanosatellites. This mission is a collaboration between the Space, Telecommunications, Astronomy, and Radiation Laboratory (STAR Lab) at the Massachusetts Institute of Technology (MIT), the Precision Space Systems Laboratory (PSSL) at the University of Florida (UF), and NASA Ames Research Center. The spacecraft provider for this mission is Blue Canyon Technologies.

## 2. CLICK-A

The first phase of the mission is the 1.2U CLICK-A terminal, designed for downlink only and hosted on a 3U spacecraft deployed from the International Space Station (ISS). This phase is intended as a risk-reduction effort for the CLICK-B/C phase of the mission. The CLICK-A terminal utilizes the same fine steering mirror (FSM), coarse acquisition camera and lens, erbium-doped fiber amplifier (EDFA), and interfaces with its host spacecraft as the CLICK-B/C terminal. The objective of the CLICK-A phase of the mission is to demonstrate  $\geq 10$  Mbps optical downlink to a 28 cm low-cost portable optical ground station, called PorTeL.<sup>6</sup> The CLICK-A terminal weighs 1.15 kg and, while transmitting, uses less than 15 W of power. The terminal transmits at 1550 nm with a M-ary pulse position modulation (M-ary PPM) format. The average optical power is 200 mW and the full angle  $1/e^2$  beam divergence is 2 mrad. The optical ground station has a 5 W 975 nm beacon as a pointing reference for the optical communication terminals. An in-depth explanation of subsystems comprising the CLICK-A terminal can be found in Serra et al.<sup>8</sup>

### 2.1 CLICK-A Flight Preparation

The CLICK-A terminal was delivered to the spacecraft provider in March 2021 and integrated into its host spacecraft in August 2021. Ground support equipment (GSE) hardware was developed to be able to test the functionality of the CLICK-A terminal. This GSE was able to measure fine pointing performance, pulse modulation, optical power, beam profile, divergence, and  $M^2$  measurement.<sup>8</sup> To be able to quickly determine whether the terminal was operating nominally without a GSE operator present, a series of self-test health check scripts were created to have the terminal check certain key functions. The self-test scripts can not test all metrics that are required to determine full functionality, with the part that could not be tested being related to the need to interface and align the optical equipment of the GSE to the terminal. The self-test scripts do test: FPGA read/write status, modulator data status, temperature sensor status, fiber optic modulator status, EDFA power and interface status, seed laser tuning status, modulator current, and heater power draw. Before each pass, the terminal runs these self-tests to report the status of the key functional systems. The self-test results are downlinked through an RF ground station network after the pass to understand what the status of the terminal was for the optical downlink experiment. These self-test scripts helped to quickly determine if any part of the terminal was not acting as expected during environmental testing.

### 2.1.1 CLICK-A Environmental Testing

At each major step in flight preparation, the terminal was checked for proper operation, which required the use of the GSE for testing its optical performance. The team had to visit the spacecraft provider’s facility to operate the ground support equipment used to verify the operation of the transmitter. The terminal was tested when it was delivered in March 2021, after integration into the host spacecraft in September 2021, post-vibration testing in November 2021, while in a thermal vacuum (TVAC) chamber at the extremes of the operating temperature range in January 2022, and post-environmental testing in March 2022. The only issue observed during this testing campaign was related to the algorithm used to tune the seed laser wavelength. At the extremes of the operating temperature range (0 °C to 45 °C), the seed laser is strained in its ability to set the wavelength of the seed laser. This tuning is critical to proper operation of the fiber Bragg grating modulation in the CLICK-A terminal.<sup>9</sup> As the payload was tested at the cold extreme of its operating temperature, the seed laser algorithm would tune to a wavelength that was not centered on the fiber Bragg grating center wavelength, causing only amplified spontaneous emission from the EDFA to be emitted from the terminal instead of amplified modulated light pulses. This issue was not observed at standard room temperature making it difficult to observe except for when the terminal was being tested in TVAC. The team was able to manually tune the seed laser to find the correct value and change the algorithm to be able to detect when it did not set the seed laser wavelength correctly. The integrated terminal passed all tests throughout the environmental testing campaign. A summary of the results can be seen in Table 1. The variation in the power at PPM4 setting was normal for the operation of the terminal as observed throughout development. The link margins for the PPM orders used by the CLICK-A terminal are shown for the post-environmental measurements in Figure 1.

Table 1: Summary of test metrics throughout CLICK-A environmental testing campaign.

Testing Phase	Power @ PPM4 (mW)	Divergence (mrad)	Link Margin @ PPM32 Apex (dB)
Pre-environmental	180	1.910	4.08
Post-vibration Test	166	1.872	10.30
TVAC Cold	163	NA	8.31
TVAC Hot	173	NA	4.00
Post-environmental	160	1.907	5.83

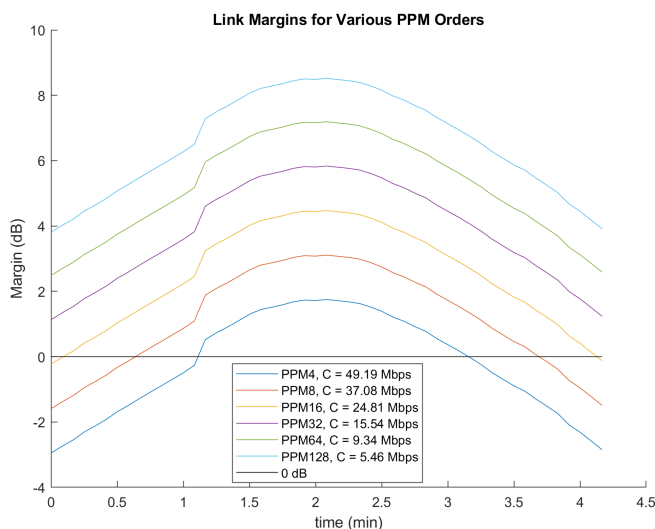


Figure 1: Post-environmental terminal link margins for the CLICK-A terminal for various PPM orders over a downlink overpass. The jump in link margin seen at the 1 min mark is the transition of the pointing, acquisition, and tracking loop from open to closed loop pointing. Image credit: Peter Grenfell

### 2.1.2 Optical Ground Station Preparation

The optical ground station at MIT Wallace Astrophysical Observatory has been undergoing preparation for operations with the CLICK-A terminal. While the PorTeL<sup>6</sup> optical ground station is designed to be portable, for simplicity of laser operations, the optical ground station is currently fixed to a pedestal mounted into the ground within an observatory shed (the roof rolls back) as shown in Figure 2a. The operators are not inside shed while the beacon laser is operating. The tracking performance has been shown to meet the mission requirements in coarse and blind pointing accuracy. The blind pointing accuracy requirement is  $\pm 100$  arcseconds RMS. The ground station demonstrated 63 arcseconds RMS in testing. The coarse pointing accuracy requirement is  $\pm 360$  arcseconds RMS and the ground station demonstrated 248 arcseconds RMS in the operational configuration. The last tracking requirement for the optical ground station has to do with the fine tracking performance of the spot on the IR camera and the APD sensor (the IR camera is used for feedback to a FSM built into the optical ground station). The fine tracking requirement is  $\pm 100$  microns (due to the 200 micron APD sensor used). The tracking performance measured in the operational configuration was demonstrated to 97.8 micron RMS.

A key part of operating the CLICK-A terminal for the demonstration downlink is for there to be a beacon laser pointing reference at the ground station for the on-orbit terminal to refine its pointing. The beacon laser selected is the Gooch and Housego EM336. The collimator paired with this laser is the Thorlabs ZC618APC-B.<sup>10</sup> The driver board for the laser has been developed and tested to demonstrate the needed optical power (5 W) to close a link with the CLICK-A terminal, as shown in Figure 2b. This driver board is also capable of sine wave modulation at the frequency that is needed to operate with the digital signal processing loop for the CLICK-B/C terminals.<sup>11</sup> The collimator has been demonstrated to achieve the necessary beam divergence needed (8.4 mrad) for closing a link with the CLICK-A terminal in laboratory testing.

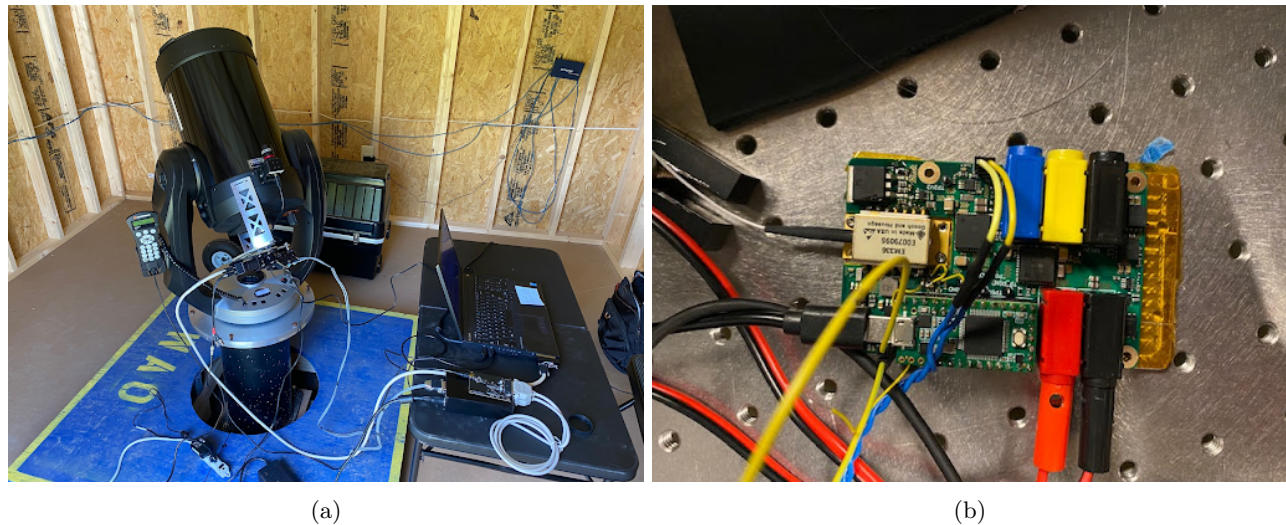


Figure 2: a) PorTeL optical ground station located within its observatory shed at MIT Wallace Astrophysical Observatory. Image credit: Peter Grenfell b) Beacon driver board for CLICK mission. Image credit: Nick Belsten

The CLICK-A spacecraft was shipped to Nanoracks in March of 2022 for integration into their deployer. The spacecraft was launched as cargo on an ISS commercial resupply mission (CRS-25) on July 15th, 2022. It is estimated that the deployment of the spacecraft will happen in September 2022.

### 3. CLICK-B/C

The second phase of the mission involves the 1.5U CLICK-B/C terminals, designed for both crosslinks and downlinks. One 3U spacecraft hosts the CLICK-B terminal and another 3U spacecraft hosts the CLICK-C terminal. The spacecraft will be deployed together from the ISS and will share the same orbital plane. The objectives of the CLICK-B/C phase of the mission are to establish a 20 Mbps intersatellite link at separations

from 25 to 580 km as well as demonstrate precision ranging at 50 cm. The CLICK-B/C terminal achieves full-duplex communications by varying the transmit and receive wavelengths for each terminal, with CLICK-B transmitting at 1537 nm and receiving at 1563 nm and CLICK-C transmitting at 1563 nm and receiving at 1537 nm. The average optical power is 200 mW and the full angle  $1/e^2$  beam divergence is 121  $\mu$ rad. The modulation format is also M-ary pulse position modulation (M-ary PPM). While operating in full-duplex mode, the terminal uses less than 35 W of power. Each terminal is equipped with a 500 mW 976 nm beacon that is sine-modulated, which is used as a pointing reference between the two terminals.

### 3.1 CLICK-B/C Optomechanical Design and Analysis

The CLICK-B/C terminal was designed to have separate sub-assemblies that could be assembled and tested without needing to fully assemble the terminal. There are four major sub-assemblies that comprise the CLICK-B/C terminal. The structure, the rear stack, the bottom stack, and the optical bench. The structure supports the other sub-assemblies in the terminal and is the mechanical interface with the host spacecraft. The rear stack sits on the back of the terminal and holds the CPU board and the FPGA board. This rear stack acts as the electrical interface between the spacecraft and the terminal as well as hosts the chip-scale atomic clock (CSAC) through the CPU board. This rear stack also hosts the high speed modulation and demodulation as well as the PAT digital signal processing through the FPGA board. The bottom stack sits on the bottom of the terminal and holds the daughter and opto-electronics boards. This bottom stack is used for all the peripheral electronics (temperature sensing, heater drivers, FSM control, EDFA control, etc.) through the daughter board, as well as the light generation and modulation through the opto-electronics board. A major difference between the CLICK-A terminal and the CLICK-B/C terminals is that the CLICK-B/C terminals implements the free space optics on a separate optical bench sub-assembly. This separate optical bench sub-assembly has many advantages, such as being able to assemble without needing access to the rest of the terminal assembly, separate thermal control of the optical bench, and ease of alignment. The optical bench assembly has an optical bench plate with certain optical mounts machined into the plate (out of a much larger piece of stock) to inherit the machine tolerance, as shown in Figure 5a. For most of the other optical mounts that interface with the optical bench, precision dowel pin holes are machined into the bench to locate the optical mounts, with further adjustment capabilities built into each of the specific optical mounts. The design of this optical layout and the mechanical tolerancing was developed with a Zemax model and an optical tolerance study to set the tolerance needed for each optic to maintain optical performance. This design process is explained more in Grenfell et al.<sup>12</sup>

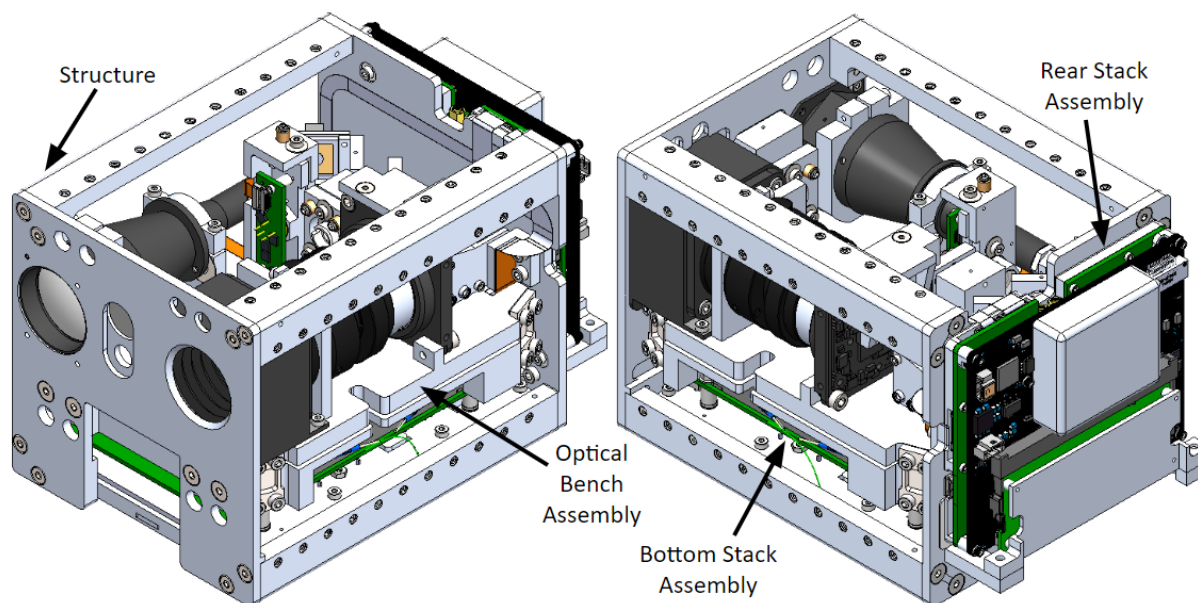


Figure 3: CLICK-B/C terminal with subassemblies labeled.

The optical design of the terminal has a 25.4 mm aperture as part of a 10.5x beam expander to achieve at least 3 dB link margin for the mission requirements. The optical bench has transmit and receive paths that are split via the different communication wavelengths of the two transceiver terminals. The fine pointing is controlled with a microelectromechanical systems fast steering mirror (MEMS FSM) with feedback through a quadrant photodiode sensor (quadcell). The transmit light enters free space through a fixed focus fiber optic collimator. The received light is sensed via an avalanche photodiode sensor (APD). The coarse pointing feedback to the spacecraft is implemented through a wide field of view camera and lens with an integrated bandpass filter for the beacon wavelength. The beacon camera optical filters are bandpass filters for the beacon wavelength, with a 10 FWHM band centered at 976 nm. There is also a baffle implemented to manage the keep-out angles of the sun and moon.<sup>12</sup> The beacon light enters free space through an adjustable fiber optic collimator (adjusted to the needed beam divergence and staked to fix the lens in place). All optics are mounted with in their mounts using RTV-566.

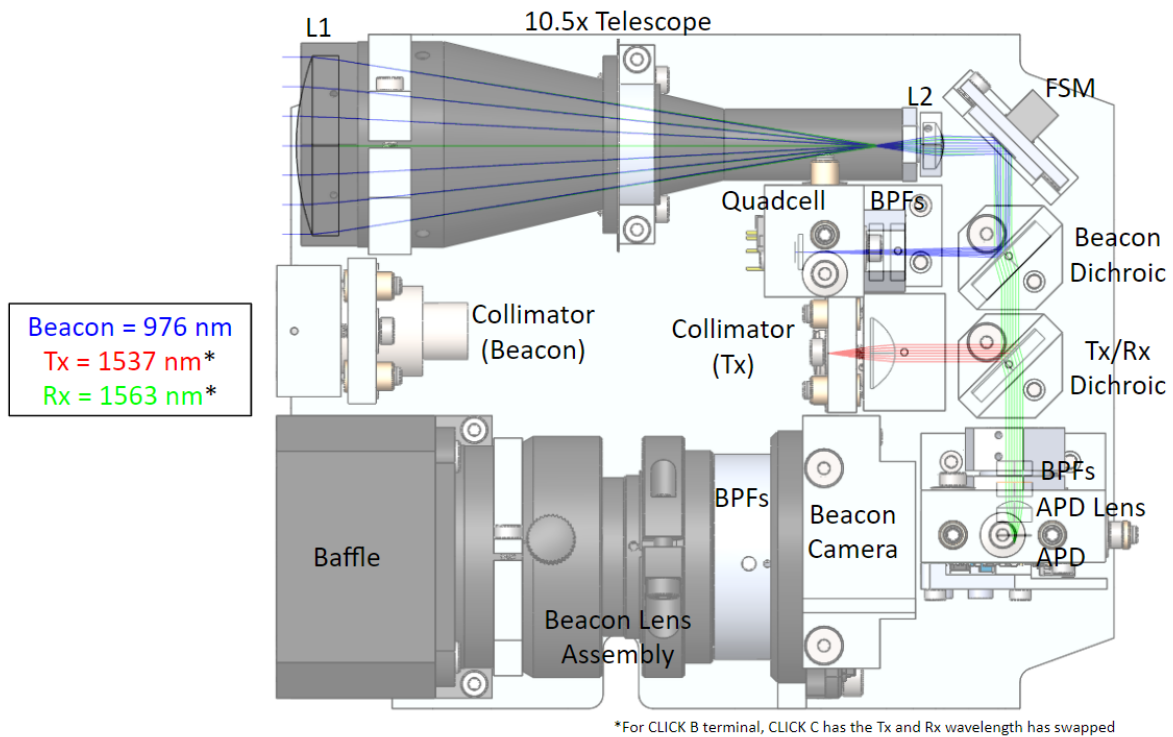


Figure 4: CLICK-B/C optical bench CAD labeled with components with optical paths overlaid. The blue lines represent the beacon light. The red lines represent the transmit light and the green lines represent the receive light.

The dichroic mounts are used to mount two separate optics. The first optic is used to split the beacon light from the receive light while the second optic is used to separate the transmit from the receive light. These dichroic mounts have a precision dowel pin hole to locate them to a precision dowel pin hole on the optical bench. These mounts also have a bolt hole to apply vertical loading to set the optical mount in place. To further prevent movement of the dichroic optical mount once it is aligned, a liquid set pin is used. A liquid set pin is another dowel pin hole machined into the optical bench, which fits into an oversized hole on the optical mount. Once the optical mount is aligned, the gap between the oversized hole and the pin is filled with 2216 epoxy to set the mount in place.

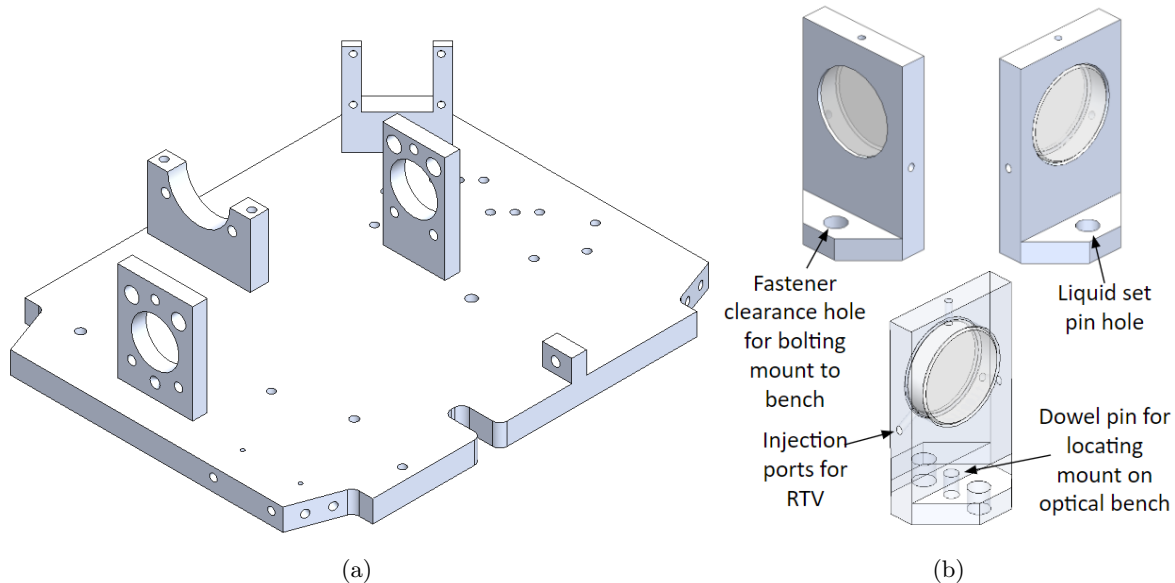


Figure 5: a) CLICK-B/C optical bench plate. b) CLICK-B/C dichroic mounts.

The quadrant photodiode (quadcell) and avalanche photodiode (APD) sensors are mounted into their respective sensor mount. Each sensor mount is supported by their own mount support which provide kinematic adjustment. The mount support is located and fixed on the bench with the same precision dowel pin, bolt down, and liquid set pin methods as the dichroic mounts. Each sensor mounts is adjustable relative to its support mount in translation normal to the direction of the light it is sensing. This adjustment is achieved through the use of Belleville washer and bolt that provide a preload against an adjustment screw. This adjustment screw is threaded into a brass insert that is press fit into the mount supports. These inserts have a fine pitch thread, which when paired with its fine pitch adjustment screw, allows for fine adjustment of the sensor mount relative to the mount support. Of the 6 degrees of freedom (DOF) that the sensor mounts have, 3 DOF (two roll DOF and one translation DOF) are constrained by the interface of the front of the sensor mount with the mount support through the front bolts of the mount support. To control of the last roll DOF and one translation DOF, two adjustment screws are used on one side of the support mount, which has a bolt with a Belleville washer to provide preload for the adjustment screw. The last translational DOF is constrained through a single adjustment screw and bolt with a Belleville washer to provide preload for the adjustment screw. This design has been iterated on due to previous prototypes not being able to constrain all DOFs with the adjustment screw arrangement. The designs shown in Figures 6 and 7 have been manufactured, assembled, and shown to control the sensor mounts as expected. The quadcell and APD mount supports also support other optical components. The quadcell mount support has a separate optical mount that holds a stack of optical filters, which threads into the mount support. The quadcell optical filters are bandpass filters for the beacon wavelength (the same as used with the camera). The APD mount support has a similar setup with a separate optical mount that threads into it, but this mount holds a stack of bandpass filters as well as the focusing lens for the APD sensor. The APD optical filters are bandpass filters for the receive light, with a 10 FWHM band centered at their receive wavelength (1563 nm for CLICK-B and 1537 nm for CLICK-C). Major redesign was needed for the APD sensor and support mount due to supplier issues for the previous APD sensor. The previous APD sensor was a Voxel RIP1-NJAF while the new APD sensor is a Laser Components IAG200H5. The implementation of this APD sensor in the receive chain of the CLICK-B/C terminal is described in detail Coogan et al.<sup>13</sup>

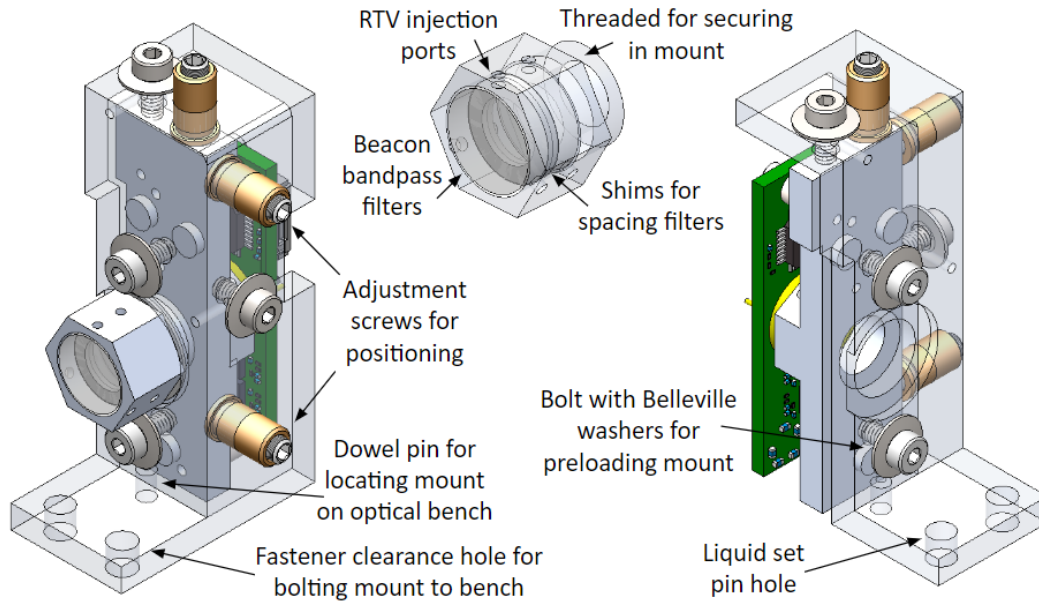


Figure 6: CLICK-B/C quadrant photodiode (quadcell) mount and mount support with labeled components.

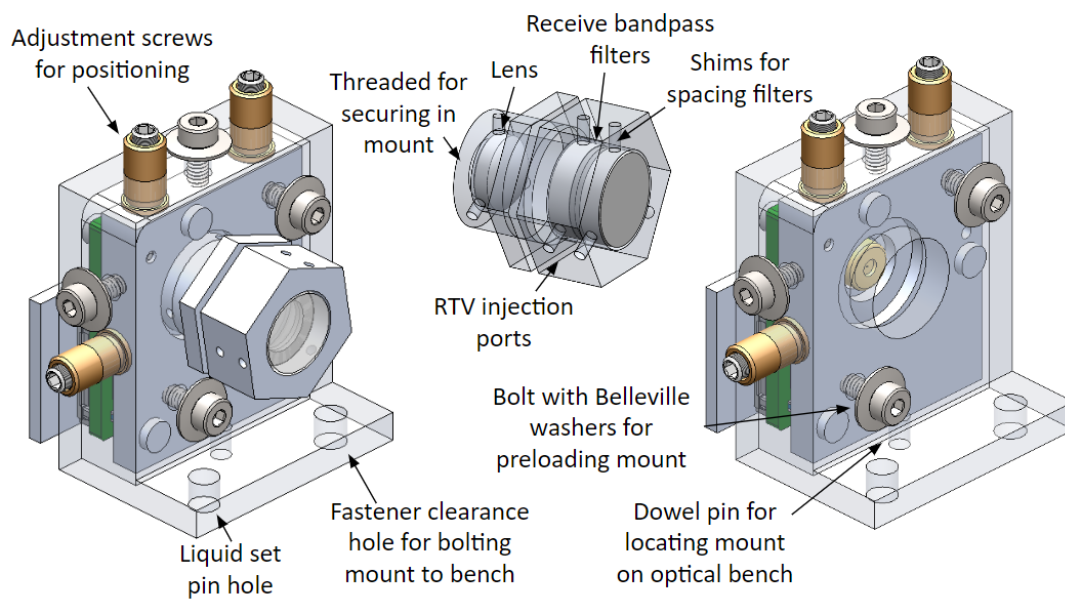


Figure 7: CLICK-B/C avalanche photodiode (APD) mount and mount support with labeled components.

There are collimators implemented on the optical bench to collimate the light from the fiber optics. The collimator mounts, as shown in Figures 8a and 8b, allow for tip/tilt adjustment. Each collimator mount hold its collimator and interfaces directly with the optical bench through the protrusions that are machined as part of the optical bench. This adjustment is designed to be similar to the sensor mounts, with an adjustment screw preloaded by a bolt with a Belleville washer. The transmit collimator is a fixed focus aspheric lens fiber optic collimator, while the beacon collimator is an adjustable focus fiber optic collimator. The mount for the beacon collimator also supports a flat fiducial mirror that is mounted relative to the beacon collimator as a reference for the spacecraft

provider to calibrate the offset between the terminal and the spacecraft star tracker. The FSM is also mounted to the optical bench in a similar protrusion off the optical bench, except it uses shims for adjustment.

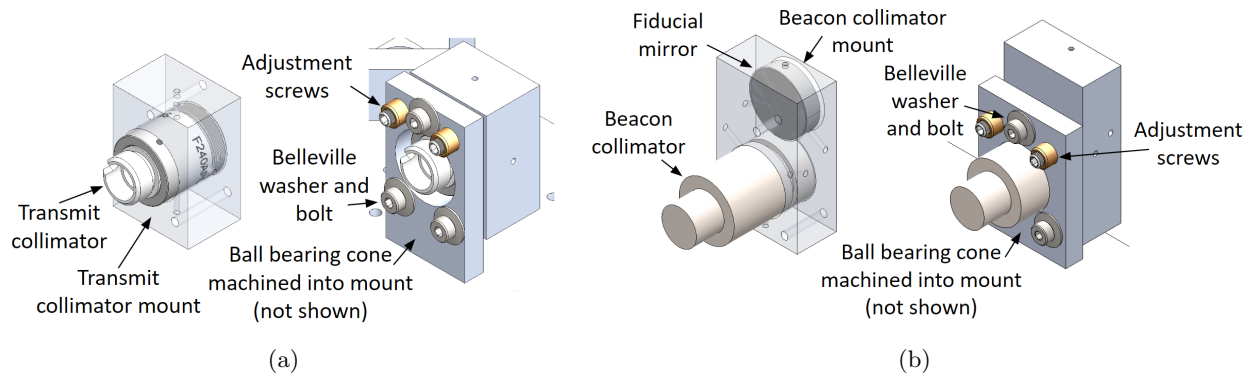


Figure 8: a) CLICK-B/C transmit collimator mount. b) CLICK-B/C beacon collimator and fiducial mirror mount.

The telescope has two lenses forming a Keplerian telescope. This telescope is used to increase the collection of the beacon and receive light as well as expand the transmit beam to reduce its divergence. The telescope and how it interfaces with the optical bench is shown in Figure 9. Due to the telescope's performance sensitivity to the relative position between L1 (the larger lens) and L2 (the small lens), the L2 lens is mounted in a threaded optical mount which threads into the telescope barrel. There is a locking nut to secure the location of the L2 lens. The L1 lens is also mounted into an optical mount that threads into the telescope barrel, but does not offer any adjustment. The telescope barrel is mounted to the optical bench through a barrel mount that is built into the optical bench. This protrusion out of the optical bench forms a cylindrical mounting face for a barrel on the telescope to fit into. This type of mount offers constraint on all DOFs except for rotation around the optical axis of the telescope as well as translation in that direction. The telescope is secured via a bolted clamp that is used to provide preload on the telescope barrel to lock it against the optical bench, as well as a collar clamp mount that slides onto and is bolted tight around the the largest part of the telescope barrel. This barrel collar clamp is mounted to the optical bench via a bolt form the underside of the bench.

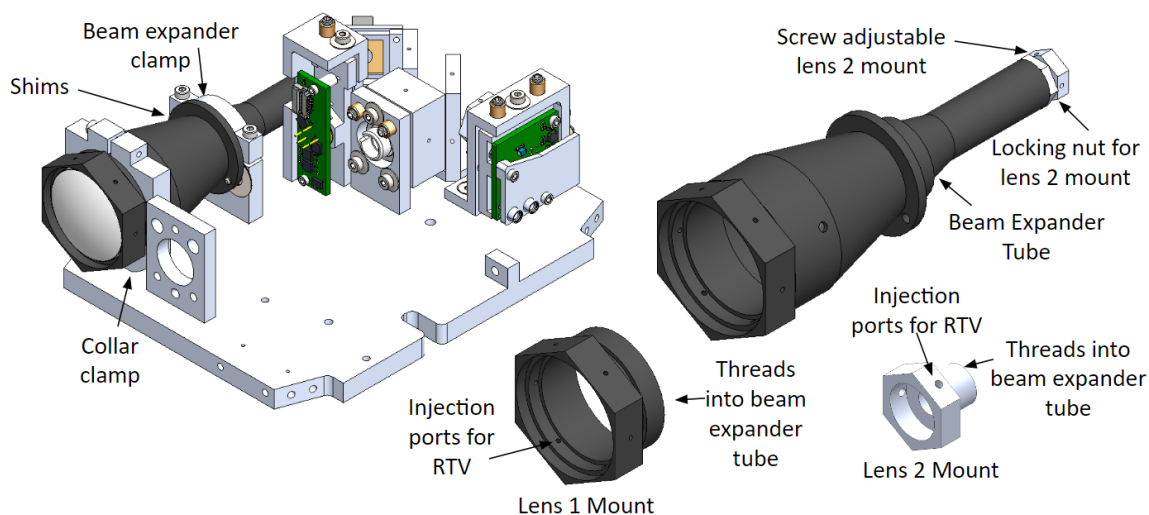


Figure 9: CLICK-B/C telescope. The black color is due to a black coating that is used for stray light reduction.

The beacon camera is mounted to the optical bench and has a custom part that is used to mount the beacon

camera lens to the camera. This custom part is another optical mount that holds the beacon bandpass filters. A baffle is implemented to reduce the stray light on the focal plane as the terminal points close to bright astronomical targets (such as the sun and the moon). The beacon camera lens is also mounted to the bench with a collar clamp that bolts tight to the barrel of the lens. This collar clamp is bolted into the optical bench. This assembly, as shown in Figure 10, provides the coarse pointing feedback to the bus to center the other terminal's beacon light on the center of the focal plane.



Figure 10: CLICK-B/C beacon camera assembly. The baffle is also coated in a black coating to reduce stray light reflections.

The interface between the optical bench and the structure is important in two aspects: thermal isolation and structural support. The optical bench is made of aluminum 6061 and thus does not have a low CTE (like titanium or Invar), which means thermal control of the optical bench is important for maintaining the alignment of the optical bench. The thermal isolators are used to mount the optical bench to the mounting plate of the EDFA, which dissipates between 5-6 W of heat during normal operation. This motivated the design of a thermal isolator that provided the maximum amount of the thermal isolation while ensuring the optical bench had a vibrational mode greater than 500 Hz. A comparison of the previous thermal isolator design to the new design is shown in Figure 11. The much longer thermal path and smaller cross-section area are what create the much lower conductance.

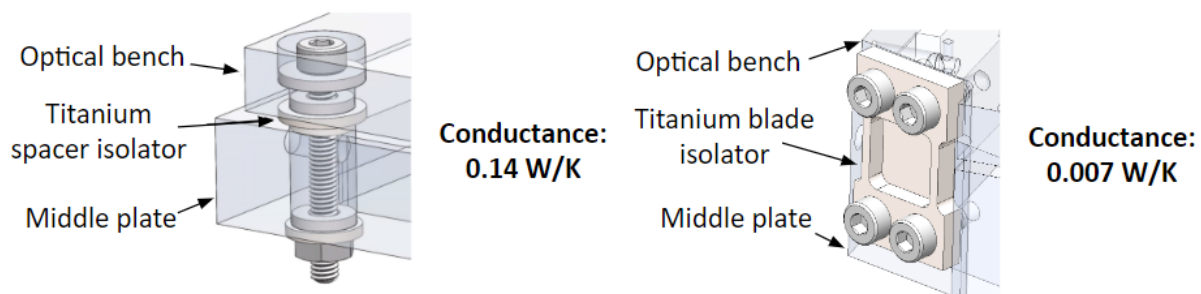


Figure 11: Comparison of the old and new thermal isolator design used to attach the optical bench sub-assembly to the structure of the terminal.

An iterative process is used to design the thermal isolator with a nominal calculated thermal isolation. The process involved designing an isolator, modifying the optical bench to interface with the middle plate through this thermal isolator, and checking its thermal and structural performance, then iterating on whether it needed more or less thermal isolation and whether the optical bench vibrational mode frequency was high enough. The

equation that defines the thermal isolation is shown in Equation 1 where  $k$  is the thermal conductivity of the material,  $A$  is the area of the conductor perpendicular to the direction of the heat flow, and  $L$  is the length of the thermal path.

$$C = \frac{kA}{L} \quad (1)$$

Due to its low thermal conduction value and high strength, 6Al-4V titanium was used in the design of the thermal isolator. To understand the impact of the new thermal isolator design on the temperature of the optical bench, the new calculated thermal isolation value was used within the terminal thermal model. The terminal is thermally modeled with Thermal Desktop, and this model shows a reduction in the maximum temperature gradient across the bench from 1.5 °C to 1.1 °C during operation when switching from the old to the new thermal isolator design. This new thermal isolator design also shows a reduction in the expected temperature range during operation (between hot and cold cases) from 30 °C to 20 °C. To understand the impact that the new thermal isolator had on the structural support of the optical bench, a structural model was built. The optical bench was determined to have a vibrational mode at 833 Hz with the new thermal isolator, which is well above the 500 Hz requirement.

### 3.2 CLICK-B/C Optomechanical Testing

An important aspect in building hardware is being able to test it to know whether it is performing as expected. Just as the CLICK-A terminal needed its own GSE to be able to know it was operating in a manner that would fulfill its mission requirements, so does the CLICK-B/C terminal. The GSE for CLICK-B/C needs to be able to test all the relevant metrics for verifying the link performance of the terminal (fine pointing performance, pulse modulation, optical power, beam profile, divergence, and  $M^2$  measurement). Figure 12 shows the block diagram for the GSE that will support the CLICK-B/C terminal.

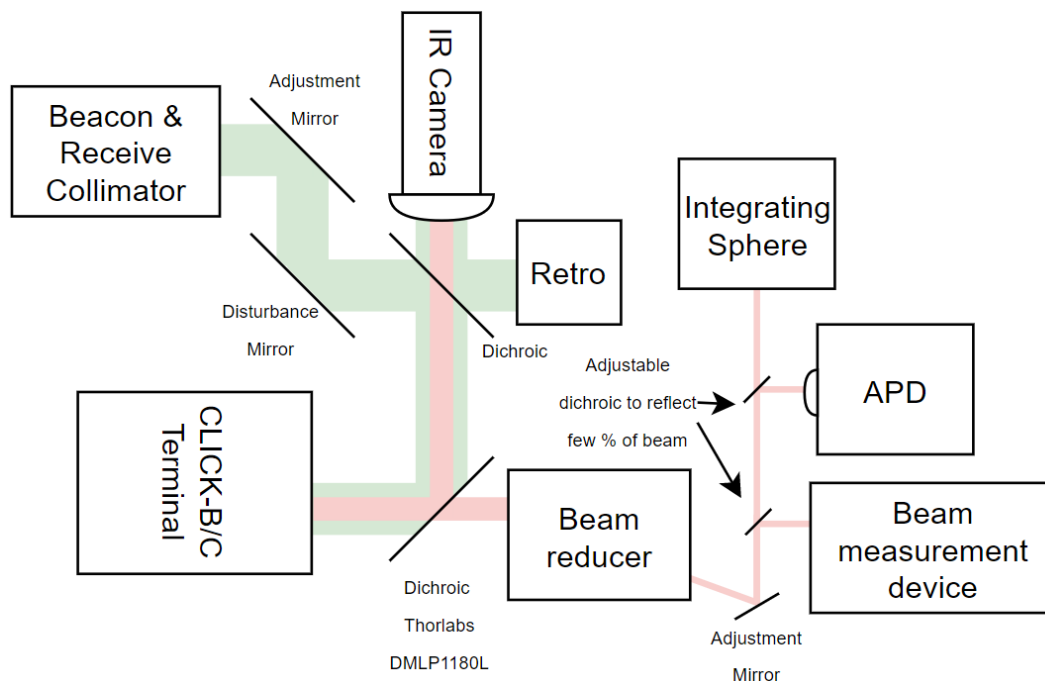


Figure 12: Block diagram of the ground support equipment for testing the CLICK-B/C terminal. The green is the beacon light and receive light. The red is the transmit light of the terminal under test.

The alignment and testing of the CLICK-B/C optical bench has an increased level of difficulty compared to the CLICK-A terminal due to its optical complexity. Since the CLICK-B/C terminal needs a much smaller beam

divergence to be able to close a link with a 2.5 cm aperture on the other crosslink terminal, the beam waist needs to be much larger. The equation for the far-field beam divergence can be seen in Equation 2, where the  $\theta$  is the beam divergence half angle,  $M^2$  is a beam quality factor (close to 1 if well-designed and aligned),  $\lambda$  is the wavelength of the light, and  $w_o$  is the beam waist. It can be seen that with the same  $M^2$  value and assuming the same 1550 nm transmit wavelength as the  $w_o$  is increased, the beam divergence angle goes down.

$$\theta = M^2 \frac{\lambda}{\pi w_o} \quad (2)$$

To produce this larger beam, the transmit light from the fixed collimator on the optical bench is input into the telescope to expand the beam by the magnification of the telescope (10.5X). To measure the far-field beam divergence of the terminal, according to ISO 11146, part of the measurement must be taken at greater than two Rayleigh lengths away from the where the beam source is. Given the large beam waist of this terminal, that would mean needing to be greater than 250 m away from the terminal properly measure the beam divergence. This beam waist is also much larger than the sensors within most lab equipment used to measure optical beam divergence. Given the large optical power values of the transmitters, this measurement needs to be measured in a laboratory environment for laser safety. To achieve the ability to measure beam divergence in lab and use it with the sensor system in lab, a beam reducer was implemented between the terminal and the beam measurement equipment. Similar test setups that needed to measure the beam properties on large optical communication terminals have utilized beam reducers for achieving a manageable beam size to work with beam measurement equipment.<sup>14</sup> This beam reducer shrinks the beam waist by its magnification. The beam reducer that was chosen is a Thorlabs BE06R, which has a magnification of six. This beam reducer brings the beam waist from 7.86 mm to 1.31 mm, and reduces the required measurement separation distance from 250.4 m to 6.95 m. The beam measurement device used was a Thorlabs BP209-IR2/M beam profiler integrated in the Thorlabs M2MS  $M^2$  measurement system.

The PAT performance of the terminal is measured in the same manner as it was for CLICK-A. This measurement, as shown in the top left of Figure 12, starts by creating a beacon reference through a large diameter refractive fiber optic collimator which is input into the terminal and aligned to the center of the quadcell sensor. There is a disturbance mirror that creates a known angular disturbance on the beacon light being input into the terminal. The disturbed beacon light is also retroreflected into a GSE camera that monitors the angular disturbance by tracking the spot of light on the focal plane of the GSE IR camera. The terminal will sense the angular disturbance of the beacon light through the quadcell, and control the FSM to correct for the disturbance. The transmitted light of the terminal will be impacted by the FSM movement and that light is input into the GSE IR camera. This light will also create a spot on the focal plane of the GSE IR camera. Tracking the center of these spots and their relative displacement in pixels can be converted to a pointing error based on the focal length of the focusing lens of the GSE IR camera and the size of the pixels on the GSE IR camera. The pulse modulation is measured via an APD sensor and oscilloscope while the optical power is measured through an integrating sphere power meter. The large diameter refractive fiber optic collimator will provide the receive light that the terminal being tested by the GSE is attempting to receive. This tests the receive capabilities of the terminal being tested.

The first aspect of testing the mounted optics of the CLICK-B/C terminal in their optical configurations is to understand the alignment process of the optical bench. The alignment process was developed over a few different iterations, but the one that gave the best results starts with aligning the transmit collimator and the optics that interact with the transmit light to the telescope. Once a sufficient alignment is achieved (by inspecting the output of the telescope via a beam profiler), the focus of the telescope is adjusted to produce the proper beam divergence. With the transmit path aligned and telescope focused, the beacon light is input into the L1 lens of the telescope and the quadcell sensor mount is translationally adjusted to center the beacon light on the quadcell. Next, the receive wavelength of that terminal is input into the telescope and the APD sensor mount is translationally adjusted to center the received light on the APD. The APD lens is adjusted to maximize power on the APD. The APD sensor mount is dithered in translation adjustment to assure that the maximum amount of the receive wavelength light is coupled onto the APD sensor.

A prototype optical bench has been manufactured and the optical components mounted in their respective mounts, as shown in Figure 13. This prototype optical bench has been tested for its far-field beam divergence with a section of the GSE outlined in Figure 14a. Light is transmitted from the EDFA fiber through full transmit optical path on the optical bench into the beam reducer. This beam reducer output was imaged and can be seen in Figure 14b. The symmetrical Gaussian shape indicates that the transmit light is not being clipped and will produce a low diverging beam with a proper focus of the telescope. The beam divergence measurement device (not shown in Figure 13) is positioned 7 meters away from the output of the beam reducer. The theoretical far-field beam divergence of the CLICK-B/C terminal is  $121 \mu\text{rad}$  based on the Zemax model. The alignment process was used and the best far-field divergence measured thus far is  $154 \mu\text{rad}$ . Testing is ongoing to improve this far-field beam divergence, but the measured beam-divergence has been calculated to achieve mission requirements with crosslinks from 25 to 580 km.

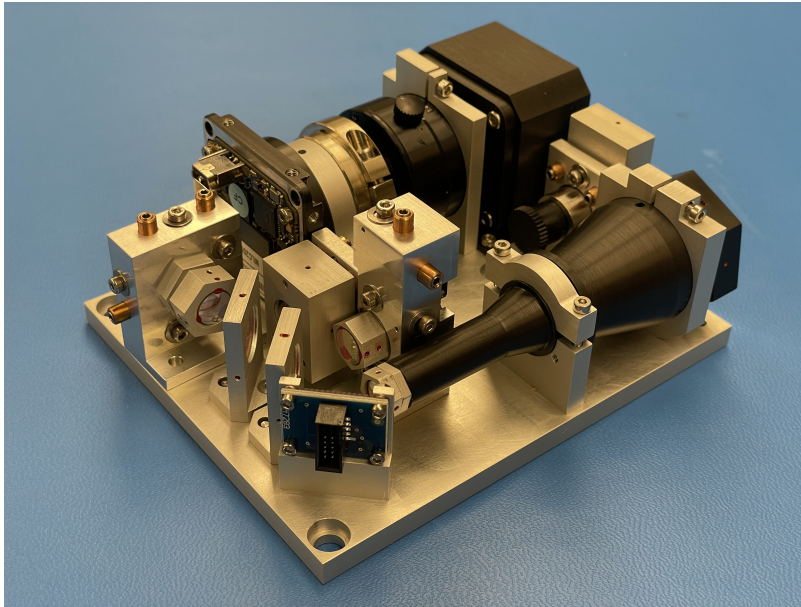


Figure 13: Prototype CLICK-B optical bench used for testing optical performance.

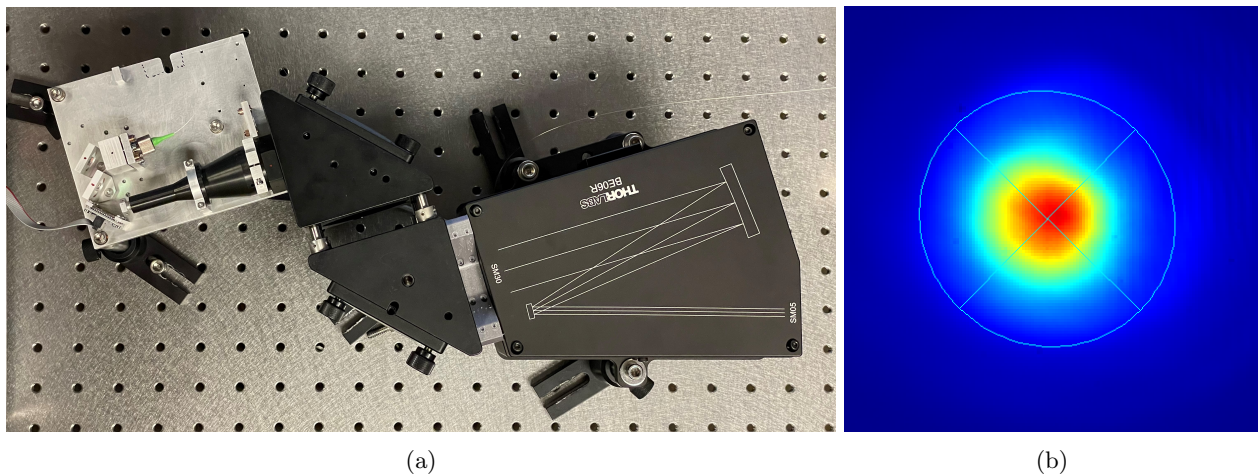


Figure 14: a) Far-field beam divergence test setup for CLICK-B/C terminal. Transmit light from the EDFA fiber is propagated through the full transmit optical path into the beam reducer. b) Beam profile of output of beam reducer with aligned optical bench.

The next step of testing the optical bench will be aligning the beacon light to the quadcell and measuring the centroiding precision of the aligned optical bench with the quadcell sensor. Once this is performed and the electronics and software to support the control of the FSM are running, a pointing, acquisition, and tracking (PAT) performance test will be performed to measure the pointing performance of the terminal. Last, the receive light optical path will be aligned and the APD receive performance will be tested. Ultimately, the separate optical test setups used to individually test each aspect of the optical bench will need to be combined into one GSE assembly that will need to travel with the CLICK-B/C terminals as they are integrated and tested, like was done for the CLICK-A terminal.

As for the rest of the assembly, most of the bottom and rear stack assemblies have been procured and test assembled for eventual integration into an engineering development unit (EDU). The procurement of the EDU and flight model (FM) optical bench components is ongoing. The lessons learned throughout the build up of the prototype optical bench have been integrated into the EDU and FM optical benches. The EDU will be environmentally tested for preparation for flight model builds. The EDU is expected to be assembled and tested by the end of 2023. The flight model terminals for CLICK-B and CLICK-C are expected to be assembled and tested in spring 2023 and then will be delivered to the spacecraft provider. The launch of the CLICK-B & C terminals will also happen through an ISS cargo resupply mission and is expected in late 2023.

#### 4. CONCLUSION

Optical communications will play an important role in expanding the communication and ranging capabilities of small satellites. The CLICK mission will advance the state of the art in optical downlinks and crosslinks for nanosatellites. The CLICK-A terminal has been integrated into its host spacecraft and successfully tested throughout an environmental testing campaign. The integrated spacecraft was launched to the International Space Station with deployment expected in September of 2022. The PorTeL optical ground station has been tested to meet its requirements and prepared for operations with CLICK-A. The CLICK-B/C assembly has been designed with four main sub-assemblies, with one being a separate optical bench. Testing of a prototype optical bench, through part of the developed optical GSE, for its far-field divergence has progressed with a measured value of  $154 \mu\text{rad}$ . The CLICK-B/C development is progressing with the build up of an engineering development unit (EDU) leading to flight model builds. Launch of the CLICK-B & C terminals is expected in late 2023.

#### ACKNOWLEDGMENTS

The CLICK mission is a collaboration between the MIT Space, Telecommunications, Astronomy, and Radiation (STAR) Lab, University of Florida's Precision Space Systems Lab (PSSL), and NASA Ames Research Center (ARC). This work was funded by the CLICK (CubeSat Laser Infrared Crosslink) Technology Demonstration Mission, Grant Number 80NSSC18K1579. The views, opinions, and/or findings contained in this work are those of the authors and should not be interpreted as representing the official views or policies, either expressed or implied, of the National Aeronautics and Space Administration.

#### REFERENCES

- [1] Blackwell, W. J., Braun, S., Bennartz, R., Velden, C., DeMaria, M., Atlas, R., Dunion, J., Marks, F., Rogers, R., Annane, B., and Leslie, R. V., "An overview of the TROPICS NASA Earth Venture Mission," *Quarterly Journal of the Royal Meteorological Society* **144**, 16–26 (Nov. 2018).
- [2] Schieler, C. M., Riesing, K. M., Bilyeu, B. C., Robinson, B. S., Wang, J. P., Roberts, W. T., and Piazzolla, S., "TBIRD 200-Gbps CubeSat Downlink: System Architecture and Mission Plan," in [*2022 IEEE International Conference on Space Optical Systems and Applications (ICSOS)*], 181–185, IEEE, Kyoto City, Japan (Mar. 2022).
- [3] Lambert, S. and Casey, W., [*Laser communications in space*], Artech House (1995).
- [4] Hemmati, H., [*Near-earth laser communications*], CRC Press (2021).
- [5] Cahoy, K., Grenfell, P., Crews, A., Long, M., Serra, P., Nguyen, A., Fitzgerald, R., Haughwout, C., Diez, R., Aguilar, A., Conklin, J., Payne, C., Kusters, J., Sackier, C., LaRocca, M., and Yenchesky, L., "The CubeSat Laser Infrared Crosslink Mission (CLICK)," in [*International Conference on Space Optics — ICSO 2018*], Karafolas, N., Sodnik, Z., and Cugny, B., eds., 33, SPIE, Chania, Greece (July 2019).

- [6] Riesing, K., *Portable Optical Ground Stations for Satellite Communication*, PhD thesis, MIT (2018).
- [7] Brown, C., “Reducing data latency with intersatellite links,” CubeSat Developers Workshop (2021).
- [8] Serra, P. C., Tomio, H., Cierny, O., Kammerer, W., Grenfell, P., Gunnison, G., Kusters, J., Payne, C., Pereira, P. d. V., Mayer, D., Stupl, J., Hanson, J., Barke, S., Clark, M., Ritz, T., Coogan, D., Conklin, J., and Cahoy, K. L., “CubeSat laser infrared crosslink mission status,” in [*International Conference on Space Optics — ICSO 2020*], **11852**, 1443–1456, SPIE (June 2021).
- [9] Kingsbury, R., *Optical Communications for Small Satellites*, PhD thesis, MIT (2015).
- [10] Cierny, O., Serra, P., Kammerer, W., Grenfell, P., Gunnison, G., Kusters, J., Payne, C., do Vale Pereira, P., Cahoy, K., Ritz, T., Conklin, J., Mayer, D., Stupl, J., and Hanson, J., “Testing of the cubesat laser infrared crosslink (click-a) payload,” Small Satellite Conference (2020).
- [11] Serra, P., Cierny, O., Diez, R., Grenfell, P., Kammerer, W., Kusters, J., Payne, C., Murphy, J., Sevigny, T., do Vale Pereira, P., Yenchesky, L., Cahoy, K., Clark, M., Ritz, T., Coogan, D., Conklin, J., Mayer, D., Stupl, J., and Hanson, J., “Optical communications crosslink payload prototype development for the cubesat laser infrared crosslink (click) mission,” Small Satellite Conference (2019).
- [12] Grenfell, P., Serra, P., Cierny, O., Kammerer, W., Gunnison, G., Kusters, J., Payne, C., Cahoy, K., Clark, M., Ritz, T., Coogan, D., Conklin, J., Mayer, D., Stupl, J., and Hanson, J., “Design and prototyping of a nanosatellite laser communications terminal for the cubesat laser infrared crosslink (click) b/c mission,” Small Satellite Conference (2020).
- [13] Coogan, D., Conroy, J., Clark, M., Conklin, J., Tomio, H., Kammerer, W., Grenfell, P., Cierny, O., Linday, C., Garcia, M., Serra, P., Cahoy, K., Stupl, J., Mayer, D., and Hanson, J., “Development of cubesat spacecraft-to-spacecraft optical link detection chain for the click-b/c mission,” Small Satellite Conference (2022).
- [14] DeVoe, C. E., Pillsbury, A. D., Khatri, F., Burnside, J. M., Raudenbush, A. C., Petrilli, L. J., and Williams, T., “Optical overview and qualification of the LLCDC space terminal,” in [*International Conference on Space Optics — ICSO 2014*], Cugny, B., Sodnik, Z., and Karafolas, N., eds., 134, SPIE, Tenerife, Canary Islands, Spain (Nov. 2017).